



*J. Serb. Chem. Soc.* 86 (1) 91–102 (2021)  
JSCS–5406

## Solid–liquid phase equilibria of $\text{H}_2\text{O}$ – $\text{Mn}(\text{H}_2\text{PO}_2)_2$ – $\text{MnCl}_2$ – $\text{NaCl}$ , $\text{H}_2\text{O}$ – $\text{Mn}(\text{H}_2\text{PO}_2)_2$ – $\text{MnCl}_2$ and $\text{H}_2\text{O}$ – $\text{NaCl}$ – $\text{MnCl}_2$ systems at 323.15 K

VEDAT ADIGUZEL\*

*Department of Chemical Engineering, Kafkas University, Kars 36100, Turkey*

(Received 21 May, revised 25 August, accepted 5 September 2020)

**Abstract:** The solid–liquid phase equilibria (SLE) and densities of  $\text{H}_2\text{O}$ – $\text{NaCl}$ – $\text{MnCl}_2$ – $\text{Mn}(\text{H}_2\text{PO}_2)_2$  quaternary system and  $\text{H}_2\text{O}$ – $\text{NaCl}$ – $\text{MnCl}_2$  and  $\text{H}_2\text{O}$ – $\text{MnCl}_2$ – $\text{Mn}(\text{H}_2\text{PO}_2)_2$  ternary systems were investigated at 323.15 K by the isothermal solution saturation method. The analyses of the liquid and solid phases were used to determine the composition of the solid phase using the Schreinemakers graphic method. The ternary systems contain one invariant point, two invariant curves and two crystallization regions. In the quaternary system, there is one invariant point, three invariant curves and three crystallization areas corresponding to  $\text{NaCl}$ ,  $\text{MnCl}_2 \cdot 4\text{H}_2\text{O}$  and  $\text{Mn}(\text{H}_2\text{PO}_2)_2 \cdot \text{H}_2\text{O}$ . The crystallization area of  $\text{Mn}(\text{H}_2\text{PO}_2)_2 \cdot \text{H}_2\text{O}$ , being the largest in comparison with those of other salts, occupied 80.75 % of the total crystallization area.

**Keywords:** manganese hypophosphite; manganese chloride; ternary system; Schreinemakers method; density.

### INTRODUCTION

Apart from being environmentally friendly, the metal hypophosphite salts  $\text{M}(\text{H}_2\text{PO}_2)_n$  draw great attention, due to their high thermal and chemical stabilities, good reducing, and mechanical features.<sup>1</sup> These salts are used as reductive, antioxidant, anticorrosive, animal feed, flame retardant in polymer, medicine, metal and food industry.<sup>1–7</sup>

$\text{Mn}(\text{H}_2\text{PO}_2)_2$  is used as a chemical intermediate in pharmacy and polymer technology, and to increase fiber quality in nylon carpet fiber production.<sup>4,5</sup> In a study, Yang *et al.* has determined that  $\text{Mn}(\text{H}_2\text{PO}_2)_2$  has high flame-retardant effect.<sup>2</sup>

In laboratory synthesis the hypophosphites are generally synthesized from sulphate, hydroxide, oxide, and nitrates of metals. The synthesis of hypophos-

\* Corresponding author. E-mail: vedatnursen@gmail.com  
<https://doi.org/10.2298/JSC200521059A>



phites obtained from hydroxides of insoluble elements in the water is generally synthesized both via multi-step reactions and expensively.<sup>4,8-15</sup>

Phase equilibria are widely used as a method in the study of equilibrium relationships. In the salt industry, they are used to increase production efficiency, and also for the recovery of valuable chemicals. Besides, they are used in the recycling and disposal of harmful wastes in terms of environmental pollution. In addition to all of these, they are used in economic synthesis by obtaining chemicals that can be synthesized by multi-step reactions in fewer reaction steps in a laboratory.<sup>16,17</sup>

In this study,  $\text{H}_2\text{O}-\text{Mn}(\text{H}_2\text{PO}_2)_2-\text{MnCl}_2-\text{NaCl}$ ,  $\text{H}_2\text{O}-\text{Mn}(\text{H}_2\text{PO}_2)_2-\text{MnCl}_2$  and  $\text{H}_2\text{O}-\text{NaCl}-\text{MnCl}_2$  systems were analyzed, and an economic method was proposed for the separation process of  $\text{Mn}(\text{H}_2\text{PO}_2)_2$  salt used in the industrial field.

SLE data of salts including  $\text{H}_2\text{PO}_2^-$  were given in Table I.<sup>8-15,18-22</sup>

TABLE I. SLE ternary and quaternary systems including  $\text{H}_2\text{PO}_2^-$

Researchers	Systems
Alisoglu and Necefoglu <sup>9</sup>	$\text{Na}^+, \text{Mn}^{2+}/\text{NO}_3^-, (\text{H}_2\text{PO}_2)^--\text{H}_2\text{O}$ at 273.15 K
Alişoglu <sup>11</sup>	$\text{K}^+, \text{Mn}^{2+}/\text{Br}^-, (\text{H}_2\text{PO}_2)^--\text{H}_2\text{O}$ at 298.15 K
Alişoglu <sup>8</sup>	$\text{Na}^+, \text{Mn}^{2+}/\text{Cl}^-, (\text{H}_2\text{PO}_2)^--\text{H}_2\text{O}$ at 298.15 K
Alişoglu <sup>10</sup>	$\text{Na}^+, \text{Mn}^{2+}/\text{Br}^-, (\text{H}_2\text{PO}_2)^--\text{H}_2\text{O}$ at 298.15 K
Alisoglu and Adıguzel <sup>12</sup>	$\text{K}^+, \text{Mn}^{2+}/\text{Br}^-, (\text{H}_2\text{PO}_2)^--\text{H}_2\text{O}$ at 298.15 K
Erge <i>et al.</i> <sup>13</sup>	$\text{Na}^+, \text{Ba}^{2+}/(\text{H}_2\text{PO}_2)^--\text{H}_2\text{O}$ at 273.15 K $\text{Na}^+/\text{Cl}^-, (\text{H}_2\text{PO}_2)^--\text{H}_2\text{O}$ at 273.15 K $\text{Ba}^{2+}/\text{Cl}^-, (\text{H}_2\text{PO}_2)^--\text{H}_2\text{O}$ at 273.15 K
Adıguzel <i>et al.</i> <sup>14</sup>	$\text{Na}^+, \text{Ba}^{2+}/\text{Cl}^-, (\text{H}_2\text{PO}_2)^--\text{H}_2\text{O}$ at 273.15 K $\text{Na}^+, \text{Zn}^{2+}/(\text{H}_2\text{PO}_2)^--\text{H}_2\text{O}$ at 273.15 K $\text{Zn}^{2+}/\text{Cl}^-, (\text{H}_2\text{PO}_2)^--\text{H}_2\text{O}$ at 273.15 K
Demirci <i>et al.</i> <sup>15</sup>	$\text{Na}^+, \text{Zn}^{2+}/\text{Cl}^-, (\text{H}_2\text{PO}_2)^--\text{H}_2\text{O}$ at 273.15 K $\text{NaH}_2\text{PO}_2-\text{NaCl}-\text{H}_2\text{O}$ at 298.15 K $\text{NaH}_2\text{PO}_2-\text{Zn}(\text{H}_2\text{PO}_2)_2-\text{H}_2\text{O}$ at 298.15 K $\text{NaCl}-\text{Zn}(\text{H}_2\text{PO}_2)_2-\text{H}_2\text{O}$ at 298.15 K
Tan <i>et al.</i> <sup>18</sup>	$\text{NaH}_2\text{PO}_2-\text{NaCl}-\text{Zn}(\text{H}_2\text{PO}_2)_2-\text{H}_2\text{O}$ at 298.15 K $\text{Ca}(\text{H}_2\text{PO}_2)_2-\text{CaCl}_2-\text{H}_2\text{O}$ at 298.15 K
Cao <i>et al.</i> <sup>22</sup>	$\text{Ca}(\text{H}_2\text{PO}_2)_2-\text{NaH}_2\text{PO}_2-\text{H}_2\text{O}$ at 298.15 K $\text{Ca}(\text{H}_2\text{PO}_2)_2 + \text{CaCl}_2 + \text{H}_2\text{O}$ at 323.15 K
Gao <i>et al.</i> <sup>20</sup>	$\text{Ca}(\text{H}_2\text{PO}_2)_2 + \text{NaH}_2\text{PO}_2 + \text{H}_2\text{O}$ at 323.15 K $\text{Mg}(\text{H}_2\text{PO}_2)_2 + \text{NaH}_2\text{PO}_2 + \text{H}_2\text{O}$ at 298 K
Yin <i>et al.</i> <sup>19</sup>	$\text{Mg}(\text{H}_2\text{PO}_2)_2 + \text{MgCl}_2 + \text{H}_2\text{O}$ at 298 K
Shi <i>et al.</i> <sup>21</sup>	$\text{Ca}(\text{H}_2\text{PO}_2)_2 + \text{CaCl}_2 + \text{H}_2\text{O}$ $\text{Ca}(\text{H}_2\text{PO}_2)_2 + \text{NaH}_2\text{PO}_2 + \text{H}_2\text{O}$ $\text{Mg}(\text{H}_2\text{PO}_2)_2 + \text{NaH}_2\text{PO}_2 + \text{H}_2\text{O}$ $\text{Mg}(\text{H}_2\text{PO}_2)_2 + \text{MgCl}_2 + \text{H}_2\text{O}$

## EXPERIMENTAL

*Apparatus and reagents*

The commercial chemicals used in the study were given in Table II. The solution condition was provided with the use of pure water whose pH was 6.6 and conductivity was  $<10^{-4}$   $\text{S m}^{-1}$ .

TABLE II. Source and mass fraction concentration of the used chemicals

Chemical	CAS No	Source	Mass fraction <sup>a</sup>
NaCl	7647-14-5	Merck	0.999
$\text{MnCl}_2 \cdot 4\text{H}_2\text{O}$	13446-34-9	Merck	0.999
$\text{Mn}(\text{H}_2\text{PO}_2)_2 \cdot \text{H}_2\text{O}$	7783-16-6	Sigma-Aldrich	$\geq 0.985$
$\text{CuCl}_2 \cdot 2\text{H}_2\text{O}$	10125-13-0	Sigma-Aldrich	0.999
$\text{C}_{10}\text{H}_{14}\text{N}_2\text{Na}_2\text{O}_8$	6381-92-6	Riedel-de Haen	0.98
HCl	7647-01-0	Riedel-de Haen	0.37
$\text{K}_2\text{Cr}_2\text{O}_7$	7778-50-9	Merck	0.98
$\text{K}_2\text{CrO}_4$	7789-00-6	Merck	0.98

<sup>a</sup>Mass fraction values were measured by the supplier of the chemicals

The density analyses were detected with the device of Mettler Toledo 30PX (accuracy  $\pm 0.001$   $\text{g cm}^{-3}$ ).

The titration measurements were conducted with Hirschmann Solarus automatic burette (accuracy 0.2 %). The stable experimental temperature was provided with a Polyscience branded cooler and a mixer water bath (accuracy  $\pm 0.05$  K).

*Experimental methods*

The phase equilibria were determined according to isothermal solubility saturation method.<sup>12,15</sup>

All the experiments were carried out at atmospheric pressure (0.1025 MPa).

The general procedure of the experiment is as below:

- 1) In the ternary system, the binary system saturated solution was prepared in a water-proof isolated tube, and placed in a water bath stabilized at 323.15 K.
- 2) The second salt was added at a certain amount to this solution. The solution was stirred for one day.
- 3) The solution was kept until the phase separation was observed clearly.
- 4) Later on, the samples were obtained from solid and liquid phases, and the necessary analyses were done.
- 5) The first forth steps of the procedure were repeated until the invariant point was reached.
- 6) In quaternary systems, the process was completed with the invariant point solution of the ternary system in the first step. In the second step, the third salt was added, and the whole process was performed, respectively.

All the density measurements were taken using a density measurement device which was stabilized at 323.15 K. The measurements were carried out in triplicate, and the calibration of the device was controlled by using pure water.

The solid phase compositions were detected according to the wet residue method of Schreinmakers.<sup>12,15,23</sup>

All the tests were repeated three times for the reliability of the test results, and the results were expressed as  $\pm$  standard deviation value.

All the tables and graphics were formed after the mathematical calculations necessary for all the data were conducted, and results were interpreted.

#### Analytical methods

$\text{Cl}^{\text{-(aq)}}$ ,  $\text{H}_2\text{PO}_2^{\text{(aq)}}$  and  $\text{Mn}^{2+\text{(aq)}}$  analyses were respectively determined by the titration with standard solutions of  $\text{AgNO}_3$ ,  $\text{K}_2\text{Cr}_2\text{O}_7$  and EDTA.<sup>24,25</sup> The expanded uncertainties ( $u_T$ ) for  $\text{Mn}^{2+}$ ,  $\text{Cl}^-$  and  $\text{H}_2\text{PO}_2^-$  analyses were respectively 1.32, 2.99 and 1.92 mass % (at the level of confidence of 0.95).  $\text{Na}^+$  amounts were calculated according to the total ion balance.

### RESULTS AND DISCUSSION

#### Solubility data of $\text{H}_2\text{O}$ – $\text{MnCl}_2$ – $\text{NaCl}$ ternary system at 323.15 K

The solubility and the density values of  $\text{NaCl}$ – $\text{H}_2\text{O}$  and  $\text{MnCl}_2$ – $\text{H}_2\text{O}$  binary systems were respectively detected as 26.86 mass %  $\text{NaCl}$  and 49.54 mass %  $\text{MnCl}_2$ , 1.191  $\text{g cm}^{-3}$ , and 1.568  $\text{g cm}^{-3}$  at 323.15 K. The solid phases belonging to these compositions were found to be  $\text{NaCl}$  and  $\text{MnCl}_2 \cdot 4\text{H}_2\text{O}$ , and  $\text{NaCl}$  and  $\text{MnCl}_2$ . The  $\text{H}_2\text{O}$  compositions and the density in the invariant point of the  $\text{H}_2\text{O}$ – $\text{MnCl}_2$ – $\text{NaCl}$  system at 323.15 K were respectively 3.14, 47.48 and 49.38 mass %, and 1.583  $\text{g cm}^{-3}$ . The solid phase of the invariant point consisted of  $\text{NaCl}$  and  $\text{MnCl}_2 \cdot 4\text{H}_2\text{O}$  salts.

The solubility and density data belonging to this system are given in Table III and Figs. 1 and 2.

TABLE III. SLE data for the  $\text{H}_2\text{O}$ – $\text{MnCl}_2$ – $\text{NaCl}$  ternary system at 323.15 K; standard uncertainties ( $u$ ) are  $u(\rho) = 0.001 \text{ g cm}^{-3}$ ,  $u(T) = 0.05 \text{ K}$ ,  $u_i(P) = 5 \%$  and  $u(w) = 0.01w$ ,  $w$  is the mass fraction; N =  $\text{NaCl}$ ; M =  $\text{MnCl}_2 \cdot 4\text{H}_2\text{O}$

No.	Content, mass %				100 w of salts		$P / \text{g cm}^{-3}$	Solid phase
	Liquid phase		Solid phase		in the liquid phase			
	$\text{MnCl}_2$	$\text{NaCl}$	$\text{MnCl}_2$	$\text{NaCl}$	$\text{MnCl}_2$	$\text{NaCl}$		
1A	0.00	26.86	0.00	93.44	0.00	100	1.191	N
2	6.21	20.65	1.64	81.01	12.24	87.76	1.225	N
3	14.69	15.29	3.22	82.15	30.85	69.15	1.279	N
4	21.39	11.33	5.52	77.9	46.71	53.29	1.325	N
5	27.86	9.00	6.51	79.68	58.98	41.02	1.383	N
6	36.01	6.18	8.43	78.39	73.02	26.98	1.460	N
7E	47.48	3.14	39.76	49.82	87.54	12.46	1.583	N+M
8E	47.48	3.14	59.42	18.97	87.54	12.46	1.583	N+M
9	48.60	1.63	56.16	1.17	93.26	6.74	1.572	M
10B	49.54	0.00	58.36	0.00	100	0.00	1.568	M

In Fig. 1, there are two crystallization areas. The first one is CAE corresponding to the crystallization area of  $\text{NaCl}$ , and the second is BFE corresponding to the crystallization area of  $\text{MnCl}_2 \cdot 4\text{H}_2\text{O}$ . Point A and F are the invariant points of the binary systems of  $\text{NaCl}$ – $\text{H}_2\text{O}$  and  $\text{MnCl}_2$ – $\text{H}_2\text{O}$ . Point E represents the

invariant of the system. Points C and B show the amount of salt by the weight of NaCl and  $\text{MnCl}_2 \cdot 4\text{H}_2\text{O}$  salt molecules and the amount of water as hydrate, respectively. The areas of AEB0 and CEBD represent the unsaturated and saturated solutions of both salts, respectively. The curves AE and EB represent the saturation curves of NaCl and  $\text{MnCl}_2$ , respectively.

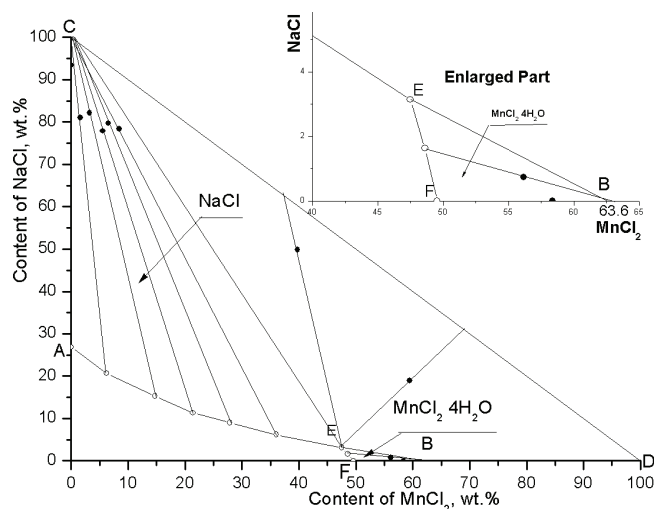


Fig. 1. SLE diagram for the  $\text{H}_2\text{O}-\text{MnCl}_2-\text{NaCl}$  ternary system at 323.15 K.

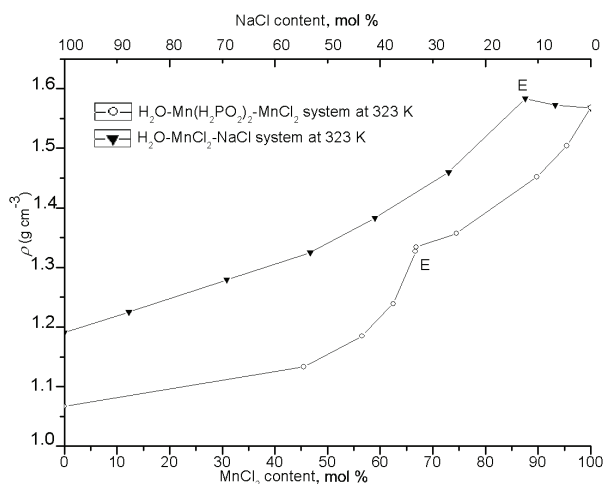


Fig. 2. Density vs. composition diagram for the ternary systems at 323.15 K.

#### Solubility data of $\text{H}_2\text{O}-\text{MnCl}_2-\text{Mn}(\text{H}_2\text{PO}_2)_2$ ternary system at 323.15 K

The solubility and density values of  $\text{Mn}(\text{H}_2\text{PO}_2)_2-\text{H}_2\text{O}$  and  $\text{MnCl}_2-\text{H}_2\text{O}$  binary systems were respectively detected as 11.14 mass %  $\text{Mn}(\text{H}_2\text{PO}_2)_2$  and

49.54 mass %  $\text{MnCl}_2$ , 1.067 and  $1.568 \text{ g cm}^{-3}$  at 323.15 K. The solid phases belonging to these compositions were found as  $\text{Mn}(\text{H}_2\text{PO}_2)_2 \cdot \text{H}_2\text{O}$  and  $\text{MnCl}_2 \cdot 4\text{H}_2\text{O}$ .

$\text{Mn}(\text{H}_2\text{PO}_2)_2$ ,  $\text{MnCl}_2$  and  $\text{H}_2\text{O}$  compositions and the density in the invariant point of  $\text{H}_2\text{O} + \text{MnCl}_2 + \text{Mn}(\text{H}_2\text{PO}_2)_2$  system at 323.15 K were respectively 15.34, 21.02 and 63.64 mass % and  $1.334 \text{ g cm}^{-3}$ . The solid phase of the invariant point consists of  $\text{Mn}(\text{H}_2\text{PO}_2)_2 \cdot \text{H}_2\text{O}$  and  $\text{MnCl}_2 \cdot 4\text{H}_2\text{O}$  salts. The solubility and density data belonging to this system are given in Table IV and Fig. 2 and 3.

TABLE IV. SLE data for the  $\text{H}_2\text{O}-\text{MnCl}_2-\text{Mn}(\text{H}_2\text{PO}_2)_2$  ternary system at 323.15 K; standard uncertainties,  $u$ , are  $u(\rho) = 0.001 \text{ g cm}^{-3}$ ,  $u(T) = 0.05 \text{ K}$ ,  $u_r(P) = 5 \%$  and  $u(w) = 0.01w$ ,  $w$  is the mass fraction; M –  $\text{MnCl}_2 \cdot 4\text{H}_2\text{O}$ ; H –  $\text{Mn}(\text{H}_2\text{PO}_2)_2 \cdot \text{H}_2\text{O}$

No.	Content, mass %				100w of salts in liquid phase		$\rho$ $\text{g cm}^{-3}$	Solid phase
	Liquid phase		Solid phase		$\text{MnCl}_2$	$\text{Mn}(\text{H}_2\text{PO}_2)_2$		
	$\text{MnCl}_2$	$\text{Mn}(\text{H}_2\text{PO}_2)_2$	$\text{MnCl}_2$	$\text{Mn}(\text{H}_2\text{PO}_2)_2$				
1A	0.00	11.14	0.00	90.13	0.00	100	1.067	H
2	6.73	11.77	0.58	88.57	45.45	54.55	1.133	H
3	11.07	12.50	1.2	84.72	56.55	43.45	1.185	H
4	15.02	13.26	3.4	74.58	62.46	37.54	1.239	H
5	20.76	15.23	2.83	82.42	66.72	33.28	1.327	H
6E	21.02	15.34	28.02	52.46	66.82	33.18	1.334	H+M
7E	21.02	15.34	56.35	32.15	66.82	33.18	1.334	H+M
8	25.1	12.63	50.29	4.13	74.48	25.52	1.357	M
9	36.7	6.17	55.24	1.91	89.75	10.25	1.452	M
10	43.4	3.03	56.09	0.91	95.46	4.54	1.504	M
11F	49.54	0.00	60.86	0.00	100	0.00	1.568	M

In Fig. 3, there are two crystallization areas. The first one is HAE corresponding to the crystallization area of  $\text{Mn}(\text{H}_2\text{PO}_2)_2 \cdot \text{H}_2\text{O}$ , and the second is BFE corresponding to the crystallization area of  $\text{MnCl}_2 \cdot 4\text{H}_2\text{O}$ . Point A and F are the invariant points of the binary systems of  $\text{Mn}(\text{H}_2\text{PO}_2)_2-\text{H}_2\text{O}$  and  $\text{MnCl}_2-\text{H}_2\text{O}$ . Point E represents the invariant of the system.

Point H and Point B show the amount of salt by weight of  $\text{Mn}(\text{H}_2\text{PO}_2)_2 \cdot \text{H}_2\text{O}$  and  $\text{MnCl}_2 \cdot 4\text{H}_2\text{O}$  salt molecules and the amount of water as hydrate, respectively. The areas of AEF0 and CHEBD represent the unsaturated and saturated solutions of both salts, respectively. The curves AE and EF represent the saturation curves of  $\text{Mn}(\text{H}_2\text{PO}_2)_2$  and  $\text{MnCl}_2$ , respectively.

#### *Solubility data of $\text{H}_2\text{O}-\text{Mn}(\text{H}_2\text{PO}_2)_2-\text{NaCl}-\text{MnCl}_2$ system at 323.15 K*

The solubility data belonging to the quaternary system are given in Table V and Fig. 4.

The invariant point data of  $\text{H}_2\text{O}-\text{Mn}(\text{H}_2\text{PO}_2)_2-\text{NaCl}$  system are 69.52, 6.02 and 24.46 mass %, respectively.

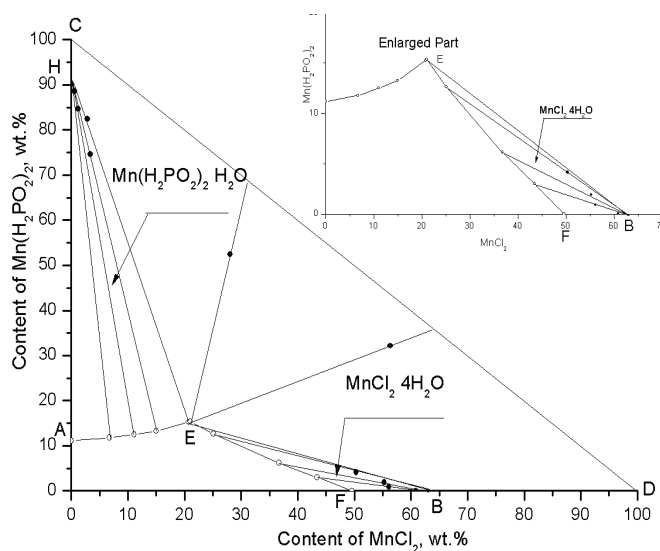


Fig. 3. SLE diagram for the  $\text{H}_2\text{O}-\text{MnCl}_2-\text{Mn}(\text{H}_2\text{PO}_2)_2$  ternary system at 323.15 K.

TABLE V. SLE data for the quaternary  $\text{H}_2\text{O}-\text{Mn}(\text{H}_2\text{PO}_2)_2-\text{NaCl}-\text{MnCl}_2$  system at 323.15 K; Jänecke index ( $J$ ) = mol per 100 mol of dry salt ( $2\text{Na}^+ + \text{Mn}^{2+}$ ); standard uncertainties ( $u$ ) are  $u(\rho) = 0.001 \text{ g cm}^{-3}$ ,  $u(T) = 0.05 \text{ K}$ ,  $u_r(P) = 5 \%$  and  $u(w) = 0.01w$ ,  $w$  is the mass fraction, N – NaCl; M –  $\text{MnCl}_2 \cdot 4\text{H}_2\text{O}$ ; H –  $\text{Mn}(\text{H}_2\text{PO}_2)_2 \cdot \text{H}_2\text{O}$

No	$100w$				$100J$			Solid phase
	$\text{Mn}^{2+}$	$\text{Na}^+$	$\text{Cl}^-$	$\text{H}_2\text{PO}_2^-$	$\text{Mn}^{2+}$	$2\text{Cl}^-$	$\text{H}_2\text{O}$	
1	20.73	1.23	28.63	0.00	93.98	99.90	680.67	N+M
2	18.28	2.37	26.60	1.19	86.58	97.60	746.93	N+M
3	16.08	2.59	23.94	1.47	83.85	96.73	891.89	N+M
4E	14.28	2.95	21.91	1.95	80.19	95.33	1011.86	N+M+H
5	13.72	0.00	11.83	10.78	100	66.80	1419.43	M+H
6	13.29	1.45	16.26	5.73	88.46	83.85	1288.10	M+H
7	12.76	2.00	17.62	3.52	84.21	90.05	1293.63	M+H
8E	14.28	2.95	21.91	1.95	80.19	95.33	1011.86	N+M+H
9	1.79	9.61	14.85	4.23	13.46	86.62	1601.20	H+N
10	4.32	7.36	14.94	3.67	32.91	88.22	1625.10	H+N
11	5.49	7.02	15.97	3.59	39.54	89.10	1496.39	H+N
12	7.57	4.76	15.73	2.53	57.07	91.87	1600.66	H+N
13E	14.28	2.95	21.91	1.95	80.19	95.33	1011.86	N+M+H

The invariant point data of  $\text{H}_2\text{O}-\text{Mn}(\text{H}_2\text{PO}_2)_2-\text{NaCl}-\text{MnCl}_2$  quaternary system are respectively 58.89, 2.77, 7.5 and 30.84 mass %.

In Fig. 4, there are three crystallization areas. The first one is AECH corresponding to the crystallization area of  $\text{Mn}(\text{H}_2\text{PO}_2)_2 \cdot \text{H}_2\text{O}$ , the second one is DBEA corresponding to the crystallization area of NaCl, and the third is BECF corresponding to the crystallization area of  $\text{MnCl}_2 \cdot 4\text{H}_2\text{O}$ . Points A, B and C are the

invariant points of the ternary systems. Point E represents the invariant of the quaternary system.

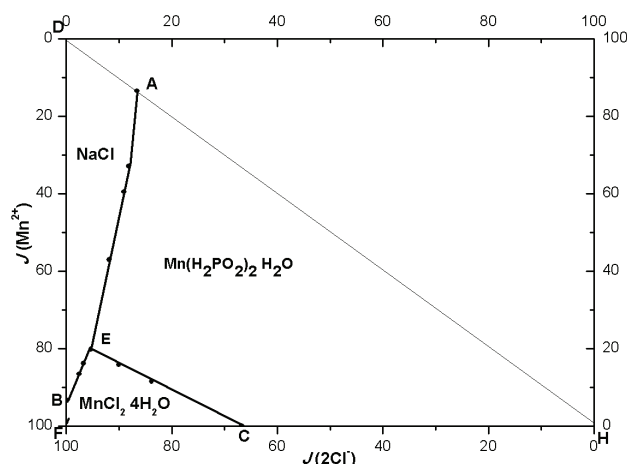


Fig. 4. SLE diagram for the  $\text{H}_2\text{O}-\text{Mn}(\text{H}_2\text{PO}_2)_2-\text{NaCl}-\text{MnCl}_2$  system at 323.15 K.

As it is seen in Fig. 4, which shows the crystallization area of the quaternary system,  $\text{Mn}(\text{H}_2\text{PO}_2)_2$  80.75 %, NaCl 11.63 %, and  $\text{MnCl}_2$  7.62 % cover the area. These values were obtained by calculating the area of the DFH triangle in Fig. 4. When the study is compared with literature data of the binary, ternary and quaternary systems, it is seen that the solubility of  $\text{Mn}(\text{H}_2\text{PO}_2)_2$  and NaCl in binary systems slightly change with the increase of temperature, but the solubility of  $\text{MnCl}_2$  increases significantly with the increase in temperature.<sup>26</sup>

The solubility of  $\text{MnCl}_2$  changed as respectively 49.54 and 56.1 mass % between 273 and 373 K. The solubility of NaCl changed as respectively 26.28 and 28.05 mass % between 273 and 373 K.<sup>26</sup>

There is limited data available for  $\text{Mn}(\text{H}_2\text{PO}_2)_2$  solubility. According to the data, the solubility of it is between 12.20 and 11.14 mass% at between 273 and 298K.<sup>8-12</sup>

The quaternary systems of this study and ref. 8 were compared (Fig. 5).

When the temperature increased from 298.15 to 323.15 K, the crystallization areas of NaCl and  $\text{Mn}(\text{H}_2\text{PO}_2)_2$  decreased; thus, their corresponding solubilities increased. In contrast to this, the crystallization area of  $\text{MnCl}_2$  increased and its solubility decreased.

In this study, the invariant points of the quaternary system were respectively 30.84, 7.5 and 2.77 mass% ( $\text{MnCl}_2$ , NaCl and  $\text{Mn}(\text{H}_2\text{PO}_2)_2$ ). According to this, there is mostly  $\text{MnCl}_2$  and at least  $\text{Mn}(\text{H}_2\text{PO}_2)_2$  in the solution. Because of this, these are the important data for the separation of  $\text{Mn}(\text{H}_2\text{PO}_2)_2$  from the solution.



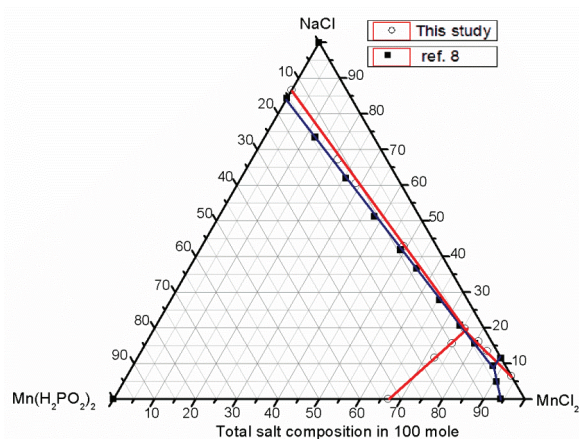


Fig. 5. Comparison of the data obtained in this study with those of reference 8 related to the same salts studied at 298.15 K.

#### CONCLUSION

Two ternary systems and one quaternary system were investigated in this study.

First of all, in the  $\text{MnCl}_2$ – $\text{NaCl}$ – $\text{H}_2\text{O}$  system,  $\text{NaCl}$  solubility reduced from 26.86 to 3.14 mass % in the existence of  $\text{MnCl}_2$ , and  $\text{MnCl}_2$  solubility reduced from 49.54 to 47.48 mass % in the existence of  $\text{NaCl}$ . It is clearly seen that  $\text{MnCl}_2$  has a sharp salting-out effect on  $\text{NaCl}$ . The density of the invariant point was determined as  $1.583 \text{ g cm}^{-3}$ .

Secondly, in  $\text{MnCl}_2$ – $\text{Mn}(\text{H}_2\text{PO}_2)_2$ – $\text{H}_2\text{O}$  system, the solubility of  $\text{Mn}(\text{H}_2\text{PO}_2)_2$  increased from 11.14 to 15.34 mass % in the existence of  $\text{MnCl}_2$ , and  $\text{MnCl}_2$  decreased from 49.54 to 21.02 mass %. Here,  $\text{MnCl}_2$  has a salting-on effect on  $\text{Mn}(\text{H}_2\text{PO}_2)_2$ . The density of the invariant point was  $1.334 \text{ g cm}^{-3}$ .

Thirdly, as the crystallizing area of the quaternary system is clearly observed,  $\text{Mn}(\text{H}_2\text{PO}_2)_2$  has the greatest area with 80.75 %,  $\text{NaCl}$  follows it with 11.63 % and  $\text{MnCl}_2$  has the smallest area with 7.62 % in the solution including all the three salts.

When literature data is analyzed, it is seen that the solubility and the density of  $\text{Mn}(\text{H}_2\text{PO}_2)_2$ – $\text{H}_2\text{O}$  binary system are respectively 12.20 mass % and  $1.089 \text{ g cm}^{-3}$  at 273 K. This result was found by Alisoğlu and Necefoğlu.<sup>9</sup> Furthermore, it has been found that the solubility is 12.48 mass % and the density is  $1.086 \text{ g cm}^{-3}$  at 298 K. It is apparently seen that the solubility and the densities of  $\text{Mn}(\text{H}_2\text{PO}_2)_2$ – $\text{H}_2\text{O}$  binary system changed slightly at 273 and 298 K, but when the temperature reached 323.15 K, the solubility and the densities decreased to 11.14 mass % and  $1.067 \text{ g cm}^{-3}$ , respectively.

It has been seen in the literature that  $\text{MnCl}_2$ – $\text{H}_2\text{O}$  binary system has 43.60 mass % solubility and  $1.491 \text{ g cm}^{-3}$  density at 298 K, and 49.40 mass % sol-

ubility at 323 K. When it is compared with the data obtained from this study and the literature cited above, it can be concluded that the solubility of  $\text{MnCl}_2\text{-H}_2\text{O}$  binary system is in the range 43.60 to 49.54 mass %. Moreover, the density of the system increased from 1.491 to 1.568  $\text{g cm}^{-3}$  in parallel with the increase of the temperature.

Finally, it has been observed that solubility of  $\text{NaCl-H}_2\text{O}$  binary system at 273, 298 and 323 K is respectively 26.25, 26.42 and 26.84 mass %, and the density is 1.201, 1.199 and 1.191  $\text{g m}^{-3}$ , respectively, again.

$\text{Mn}(\text{H}_2\text{PO}_2)_2$  is obtained by a displacement reaction of  $\text{MnCl}_2$  with  $\text{NaH}_2\text{PO}_2$  in order to produce  $\text{Mn}(\text{H}_2\text{PO}_2)_2$  and  $\text{NaCl}$ . The salts can be separated from each other as a result of their solubility differences by creating  $\text{Na}^+$ ,  $\text{Mn}^{2+}/\text{Cl}^-$ ,  $(\text{H}_2\text{PO}_2)^-//\text{H}_2\text{O}$  reciprocal quaternary system. In this study, a method has been proposed for purification of  $\text{Mn}(\text{H}_2\text{PO}_2)_2$  by separating it from the solution medium by using phase equilibrium method, which enables the synthesis of  $\text{Mn}(\text{H}_2\text{PO}_2)_2$  more economically and easily than the synthesis method used in the traditional laboratory.

In the study with the same quaternary system at 298 K, it is seen that the crystallizing area of  $\text{Mn}(\text{H}_2\text{PO}_2)_2$  covers 82.9 % of the total area. A method can be proposed to separate these salts using temperature and phase changes with the joint evaluation from literature and this study. Especially, the separation of  $\text{Mn}(\text{H}_2\text{PO}_2)_2$  which has the highest crystallization area, is an important result since it is more economical than the traditional method. According to this, it has been concluded that  $\text{Mn}(\text{H}_2\text{PO}_2)_2$  can be separated via temperature change.

Therefore, this study suggests an economic method for the separation of  $\text{Mn}(\text{H}_2\text{PO}_2)_2$  which solves the least (2.77 %) and covers the most crystallizing area (80.75 %) in the solution including three salts mentioned.

*Acknowledgment.* The authors would like to thank the referees for their valuable comments, which helped to improve the manuscript.

#### ИЗВОД

РАВНОТЕЖА ФАЗА ЧВРСТО–ТЕЧНО У  $\text{H}_2\text{O-Mn}(\text{H}_2\text{PO}_2)_2\text{-MnCl}_2\text{-NaCl}$ ,  
 $\text{H}_2\text{O-Mn}(\text{H}_2\text{PO}_2)_2\text{-MnCl}_2$  И  $\text{H}_2\text{O-NaCl-MnCl}_2$  СИСТЕМИМА НА 323,15 К

VEDAT ADIGUZEL

*Department of Chemical Engineering, Kafkas University, Kars 36100, Turkey*

Равнотежа фаза чврсто–течно и густине у кватернарном систему  $\text{H}_2\text{O-NaCl-MnCl}_2\text{-Mn}(\text{H}_2\text{PO}_2)_2$ , као и у тернарним системима  $\text{H}_2\text{O-NaCl-MnCl}_2$  и  $\text{H}_2\text{O-MnCl}_2\text{-Mn}(\text{H}_2\text{PO}_2)_2$ , испитане су применом методе мерења zasiћења раствора при изотермским условима на 323,15 К. Анализом течне и чврсте фазе утврђен је састав чврсте фазе коришћењем Schreinemakers графичке методе. Тернарни системи садрже једну инваријатну тачку, две криве растворљивости и два поља кристализације. У кватернарном систему постоји једна инваријатна тачка, три криве растворљивости и три поља кристализације која одговарају чврстим фазама  $\text{NaCl}$ ,  $\text{MnCl}_2\cdot 4\text{H}_2\text{O}$  и  $\text{Mn}(\text{H}_2\text{PO}_2)_2\cdot \text{H}_2\text{O}$ .

Поље кристализације  $Mn(H_2PO_2)_2 \cdot H_2O$ , као највеће у поређењу са областима кристализације осталих чврстих фаза, заузима 80,75 % укупне површи кристализације.

(Примљено 21. маја, ревидирано 25. августа, прихваћено 5. септембра 2020)

## REFERENCES

1. W. Wu, S. Lv, X. Liu, H. Qu, H. Zhang, J. Xu, *J. Therm. Anal. Calorim.* **118** (2014) 1569 (<https://doi.org/10.1007/s10973-014-4085-8>)
2. W. Yang, W. J. Yang, B. Tawiah, Y. Zhang, L. L. Wang, S. E. Zhu, T. B. Y. Chen, A. C. Y. Yuen, B. Yu, Y. F. Liu, *Compos. Sci. Technol.* **164** (2018) 44 (<https://doi.org/10.1016/j.compscitech.2018.05.023>)
3. G. A. Bhat, P. Vishnoi, S. K. Gupta, R. Murugavel, *Inorg. Chem. Commun.* **59** (2015) 84 (<https://doi.org/10.1016/j.inoche.2015.07.006>)
4. P. Noisong, C. Danvirutai, *Spectrochim. Acta, A* **77** (2010) 890 (<https://doi.org/10.1016/j.saa.2010.08.028>)
5. P. Noisong, C. Danvirutai, T. Srithanratana, B. Boonchom, *Solid State Sci.* **10** (2008) 1598 (<https://doi.org/10.1016/j.solidstatesciences.2008.02.020>)
6. A. Suekhhayad, P. Noisong, C. Danvirutai, *J. Therm. Anal. Calorim.* **129** (2017) 123 (<https://doi.org/10.1007/s10973-017-6156-0>)
7. Y. Zeng, J. Yi, H. Wang, G. Zhou, S. Liu, *J. Mol. Struct. THEOCHEM* **724** (2005) 81 (<https://doi.org/10.1016/j.theochem.2005.03.014>)
8. V. Alisoğlu, *C.R. Chim.* **5** (2002) 547 ([https://doi.org/10.1016/S1631-0748\(02\)01411-X](https://doi.org/10.1016/S1631-0748(02)01411-X))
9. V. Alisoglu, H. Necefoglu, *C.R. Acad. Sci., Ser. IIb: Mec., Phys., Chim., Astron.* **324** (1997) 139 ([https://doi.org/10.1016/S1251-8069\(99\)80017-7](https://doi.org/10.1016/S1251-8069(99)80017-7))
10. V. Alisoğlu, *C.R. Chim.* **8** (2005) 1684 (<https://doi.org/10.1016/j.crci.2004.11.041>)
11. V. Alisoglu, *C.R. Acad. Sci., Ser. IIc: Chim.* **1** (1998) 781 ([https://doi.org/10.1016/S1251-8069\(99\)80046-2](https://doi.org/10.1016/S1251-8069(99)80046-2))
12. V. Alisoglu, V. Adiguzel, *C.R. Chim.* **11** (2008) 938 (<https://doi.org/10.1016/j.crci.2007.12.001>)
13. H. Erge, V. Adiguzel, V. Alisoglu, *Fluid Phase Equilib.* **344** (2013) 13 (<https://doi.org/10.1016/j.fluid.2012.12.033>)
14. V. Adiguzel, H. Erge, V. Alisoglu, H. Necefoglu, *J. Chem. Thermodyn.* **75** (2014) 35 (<https://doi.org/10.1016/j.jct.2014.04.014>)
15. S. Demirci, V. Adiguzel, Ö. Şahin, *J. Chem. Eng. Data* **61** (2016) 2292 (<https://doi.org/10.1021/acs.jced.5b00988>)
16. Y. Mastai, *Advances in Crystallization Processes*, InTech, Rijeka, 2012, pp. 400–413 (<https://doi.org/10.5772/2672>)
17. H. Civelekoğlu, R. Tolun, N. Bulutçu, *İnorganik teknolojiler*, İTÜ Maden Fakültesi Ofset Atölyesi, İstanbul, 1987, pp. 80–103 (<http://www.ituyayinlari.com.tr/kitapdetay.asp?KitapID=34&inorganik-Teknolojiler>)
18. L. Tan, J. Wang, H. Zhou, L. Wang, P. Wang, X. Bai, *Fluid Phase Equilib.* **388** (2015) 66 (<https://doi.org/10.1016/j.fluid.2014.12.047>)
19. J. Yin, X. Shi, H. Zhou, J. Tang, Y. Dai, X. Bai, *J. Chem. Eng. Data* **62** (2017) 744 (<https://doi.org/10.1021/acs.jced.6b00813>)
20. S. Gao, X. Shi, J. Yin, Z. Wan, H. Zhou, G. Li, *Fluid Phase Equilib.* **411** (2016) 7 (<https://doi.org/10.1016/j.fluid.2015.11.033>)
21. X. Shi, J. Yin, H. Zhou, X. Gu, Y. Dai, J. Tang, *J. Chem. Eng. Data* **62** (2017) 1011 (<https://doi.org/10.1021/acs.jced.6b00828>)

22. H. Cao, H. Zhou, X. Bai, R. Ma, L. Tan, J. Wang, *J. Chem. Thermodyn.* **93** (2016) 255 (<https://doi.org/10.1016/j.jct.2015.09.006>)
23. H. Schott, *J. Chem. Eng. Data* **6** (1961) 324 (<https://doi.org/10.1021/je00103a002>)
24. J. R. Van Wazer, *Phosphorus and its Compounds*, Interscience Publishers, New York, 1958, pp. 60–62 (<https://doi.org/10.1002/ange.19610731513>)
25. T. Gündüz, *Kantitatif analiz laboratuvar kitabı*, Gazi Büro Kitabevi, Ankara, 2012, pp. 280–282 (ISBN 9799757313457)
26. D. R. Lide, *CRC handbook of chemistry and physics*, CRC Press, Boca Raton, FL, 2012, pp. 468–469 (<https://doi.org/10.1080/08893110902764125>)
27. A. R. Kul, H. Erge, İ. Meydan, *Yüzüncü Yıl Üniversitesi Fen Bilim. Enstitüsü Derg.* **19** (2014) 62 (<https://dergipark.org.tr/en/download/article-file/204648>).